UNIVERSITY OF ALBERTA

Preliminary Characterization of the Tight-Junction Associated Protein ZO-1 Using Antisense mRNA Techniques

BY

Vikram Avinash Maraj

A thesis submitted to the Faculty of Graduate Studies and Research in partial fulfillment of the requirements for the degree of

Master of Science

DEPARTMENT OF ANATOMY AND CELL BIOLOGY

Edmonton, Alberta

Fall, 1994

ISBN 0-315-95072-2

Canada

THE UNIVERSITY OF ALBERTA

RELEASE FORM

NAME OF AUTHOR: VIKRAM AVINASH MARAJ

TITLE OF THESIS: PRELIMINARY CHARACTERIZATION OF THE TIGHT-JUNCTION ASSOCIATED PROTEIN ZO-1 USING ANTISENSE mRNA TECHNIQUES

DEGREE: MASTER OF SCIENCE

YEAR THIS DEGREE GRANTED FALL 1994

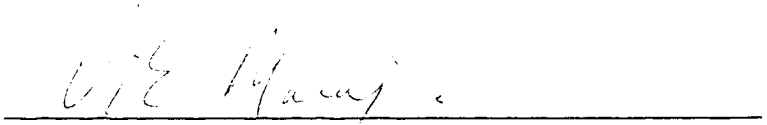

1004 Leuders Cresent
Sherwood Park, Alberta
T8A 1A9

April 14, 1994

THE UNIVERSITY OF ALBERTA

FACULTY OF GRADUATE STUDIES AND RESEARCH

The undersigned certify that they have read, and recommend to the Faculty of Graduate Studies and Research for acceptance, a thesis entitled PRELIMINARY CHARACTERIZATION OF THE TIGHT-JUNCTION ASSOCIATED PROTEIN ZO-1 USING ANTISENSE mRNA TECHNIQUES submitted by VIKRAM AVINASH MARAJ in partial fulfillment of the requirements for the degree of MASTER OF SCIENCE.

Dr. Bruce Stevenson

Dr. David Begg

Dr. Colin Rasmussen

Dr. Stephen Rice

April 14, 1994

For my sister, Ramona Maraj. It is in the spirit of Invictus that I dedicate this chapter of my life. Know that in documents, such as this, knowledge is written within lines but wisdom lies between.

ABSTRACT

A canine cDNA encoding a portion of the tight junction-associated protein ZO-1 was isolated using a rat ZO-1 homolog as a probe to screen a λ phage cDNA library. The resulting 1 kb fragment, designated as dZ3, was shown to be a portion of the canine ZO-1 cDNA by Northern blot and sequence analysis. Based on canine and human sequence information, a 1.5 kb canine cDNA, designated dZ4, was obtained using the polymerase chain reaction. dZ4 was partially sequenced, but not used in further experiments. The dZ3 cDNA was subcloned in the antisense orientation into a eukaryotic expression vector plasmid containing the hMTIIa promoter for Zn^{++}-inducible expression. This construct was co-transfected with a vector containing a neomycin selectable marker into the Madin-Darby canine kidney cell line, and resultant colonies were isolated and screened by Southern blotting for the presence of the antisense construct. One of these clones, designated A1, was used to assay the effect of antisense RNA expression on tight junction assembly using a "calcium-jump assay". Cells were grown in medium deficient in both Ca^{++} and Zn^{++} for 72 hours and then switched to medium containing both cations. The effect of antisense ZO-1 mRNA expression on tight junction formation was assessed by quantifying ZO-1 protein levels by immunoblot and measuring the development of transepithelial resistance. Results indicated that there was a positive

correlation between transepithelial resistance and ZO-1 protein levels. This preliminary evidence suggests that ZO-1 plays a role in the assembly of the tight junction.

Table of Contents

Introduction

Two characteristic features of polarized epithelial and endothelial cells are their abilities to act as a barrier between environmentally distinct compartments and to vectorially transport solutes from one compartment to another. The tight junction (TJ) circumscribes the apex of polarized epithelial cells, and acts as a semi-permeable barrier to regulate paracellular permeability. By controlling the paracellular movement of ions and other solutes, the TJ can modulate or maintain gradients established by transcellular mechanisms. The polarized distribution of apical and basolateral membrane proteins in these cells, initially mediated by intracellular sorting mechanisms (Caplan and Matlin, 1989; Rothman et al., 1990), is believed to be maintained by the tight junction (TJ). Within the plane of the plasma membrane, the TJ may act as a barrier, preventing the redistribution of certain ion channels, ion pumps, and enzymes, which characterize the apical and basolateral cell surface domains (Diamond, 1977).

The TJ is seen as discrete sites of plasma membrane contact between adjacent cells in thin section transmission electron microscopy. Freeze-fracture of fixed tissue reveals this region to be a branching array of linear fibrils appearing as ridges on the protoplasmic membrane face and complementary grooves on the exoplasmic face (Staehelin,

1974). In unfixed material, however, the junctional fibrils appear as rows of particles (Staehelin, 1973). The composition of these fibrils is undetermined.

The permeability of the TJ, a characteristic of the physiological state of a tissue, can be measured by passing a current across a cell monolayer and recording the transepithelial resistance (TER) (Diamond, 1977). This is directly proportional to the permeability of inorganic ions through the paracellular pathway. It has been suggested that cells can regulate paracellular traffic by altering the structure of the tight junction by increasing or decreasing the complexity of the fibrillar array that constitutes the tight junction. Increases in fibrillar complexity has been positively correlated with increases in TER (Claude and Goodenough, 1973; Madara et al., 1985).

Roles for both lipids and proteins in the structure and function of the TJ have been proposed. Arguments for a TJ lipid structure propose the existence of a series of protein-stabilized inverted lipid micelles (Kachar et al., 1981; Pinto da Silva, 1982), which are responsible for the junctional strands or rows of beads seen in fixed and unfixed freeze-fracture images, respectively. Evidence for this model also comes from the resemblance, in freeze-fracture, of Ca^{++}-induced phospholipid micelles, spheres comprised solely of lipids, to the TJ particles observed in freeze-fractured unfixed tissue (Verkliej, 1984). Moreover,

the application of protein synthesis inhibitors, metabolic uncouplers and cytoskeletal disrupting agents on intact cell monolayers have shown little effect on the formation of TJ-like strands (Kachar et al., 1981; Chevalier et al., 1987).

The role of proteins in the assembly of the TJ has been established by studies in which the addition of protein-synthesis inhibitors reversibly inhibited the formation of TJs in cells cultured after trypsinization (Cereijido et al., 1981; Griepp et al., 1983). The addition of inhibitor was ineffective if trypsinized cells were maintained in suspension for two hours prior to plating. These studies indicate that synthesis of proteins lost during trypsinization is required for TJ formation. The discovery of occludin (Furuse et al., 1993), a tight junction protein with many properties of an integral membrane protein, provides the first indication that the junctional fibrils are, at least in part, proteinaceous.

Other proteins localized to the tight junction have also been identified and characterized to various extents. ZO-1, an ~220 kD protein, was identified as an cytosolic membrane marker for the tight junction by Stevenson et al., (1986). Cingulin (Citi et al., 1988), discovered by raising monoclonal antibodies (mAb) against intestinal brush-border myosin, is a 140kD polypeptide which also localizes to the cytoplasmic side of the TJ. ZO-2 (Gumbiner et al., 1991), a 160 kD protein, and p130 (Balda et al., 1993) a 130 kD

protein, both co-immunoprecipitate with ZO-1 in the presence of anti-ZO-1 antibody. While ZO-2 has been shown to localize to the TJ, p130 has yet to be confirmed as tight junction-associated. Using a mAb approach, Zhong et al., (1993) were able to identify 7H6, a 155 kD peripheral membrane associated protein, which, by ultrastructural immunogold localization is specific for the tight junction. Recently, rab13, a 24 kD GTPase has been co-immunolocalized with ZO-1 at the TJ (Zahraoui et al., 1994) although confirmatory immunoelectron microscopy has not been published. Actin filaments have also been localized to the tight junction (Meza et al., 1980; Madara, 1987) and are also believed to play a role in the regulation of junctional permeability.

Of all junctional components, ZO-1 is the first and best characterized protein associated with the TJ. Using a preparation of a TJ-enriched mouse liver membrane fraction as an immunogen, a mAb, R26.4, was generated to ZO-1 (Stevenson et al., 1986). Immunoelectron microscopy localized ZO-1 to the tight junction. Further characterization has shown ZO-1 to be a phosphoprotein which displays both inter-species size variability and tissue-specific splice variation (Anderson et al., 1988; Willot et al., 1992). ZO-1 (~1700 amino acids) was also the first tight junction protein to be cloned and fully sequenced (Itoh et al., 1993; Willot et al., 1993). ZO-1 exists in two forms, designated as α^+ and α^-, which differ by 80 amino

acids (Willot et al., 1992). These two forms result from alternate mRNA splicing. Both forms localize to the TJ, but there is a differential tissue-specific localization for each. The larger α^+ form is found in many epithelial types but the smaller α^- form is detected in endothelial cells and the highly specialized junctions of glomerular epithelial cells and Sertoli cells. Moreover, freeze fracture analysis has shown a correlation between specific isoform expression and fibrillar morphology (Willot et al., 1992). These data suggest that cytosolic peripheral membrane components may affect the behavior of fibril particles. Further sequence information shows the amino terminal 763 amino acids (aa) of human ZO-1 to be partially homologous to a family of proteins involved in signal transduction at regions of cell-cell contact (Willot et al., 1993). The defining member of this family is the discs-large (dlg) tumor suppressor protein located at septate junctions within epithelial cells of the imaginal discs of Drosophila. It has been shown that mutations in the dlg gene causes neoplastic overgrowth of the imaginal discs as a consequence of disrupted apical-basolateral cell polarity and intercellular adhesion (Woods et al., 1991). The signaling events which normally operate, and are disrupted under these circumstances, are uncharacterized.

ZO-1 has been shown to be expressed in a variety of non-epithelial non-tight junction-forming cells, including

primary cultures of astrocytes (Howarth et al., 1992). Immunofluorescent microscopic data gathered by Itoh et al., (1993), indicates that ZO-1 co-localizes with cadherins in non-epithelial cell types such as fibroblasts and is present at sites of initial cell-cell contact. Moreover, it has been shown by immunoelectron microscopy that ZO-1 localizes to adherens junctions in cells of the intercalated disks of cardiac muscle (Itoh et al., 1991 and 1993). Experiments in which mouse L cells were transfected with cDNAs encoding N-, P-, and E-cadherins demonstrated by immunofluorescent co-localization that their protein products either directly or indirectly interact with ZO-1 (Itoh et al., 1993). Other data, however, indicate that the expression of E-cadherin in S180L (sarcoma) cells is not sufficient to cause a redistribution of ZO-1 even though S180L cells have been reported to form adherens type junctions in response to the expression of E-cadherin (Howarth et al., 1994; Mege et al., 1988). This result suggests that factors other than cadherins are required to localize ZO-1 to adherens junctions.

Data described above, coupled with information that ZO-1 binds tetrameres of spectrin (Itoh et al., 1991), indicate that ZO-1 may have a role in linking the cortical cytoskeleton to both the tight and adherens junctions. That the integrity of the TJ, like that of the adherens junction and desmosome (Kartenbeck et al., 1991; Volber et al.,

1986), is mediated by interactions with the cytoskeleton is indicated by the fact that application of cytochalasins cause the disruption of the actin cytoskeleton and TJ, as well as a coincident increase in paracellular permeability (Meza et al., 1982; Madara et al., 1986; Stevenson and Begg in press). Moreover, cytochalasin induced focal accumulations of the tight junction-associated protein ZO-1 aggregate along cell boundaries, and these aggregates co-localized with similarly disrupted actin in the apical ring (Stevenson and Begg, in press). These results indicate that ZO-1 is not only associated with the electron dense cytoplasmic plaque, but that the junctional plaque is connected to actin filaments.

The role of extracellular Ca^{++} in the maintenance of the TJ is well documented (Sedar and Forte, 1964; Pitelka et al., 1983; Gonzales-Mariscal et al., 1990). The effects of Ca^{++} are likely to be exerted through the Ca^{++}-dependent cell-cell adhesion molecules, cadherins. "Ca^{++} switch" assays involve preventing the formation of TJs by maintaining epithelial cells in Ca^{++}-deficient medium (<5 μm) and then switching cells to normal Ca^{++}-containing medium (1.3 mM), permitting the establishment of junctional complexes including the TJ. The level(s) at which Ca^{++} acts in the establishment of the TJ is unclear, although it is likely to be indirect. It has been shown that antibodies against the extracellular domain of the Ca^{++}-dependent cell-

cell adhesion molecule, E-cadherin retard tight junction development in a fashion similar to calcium depletion (Gumbiner et al., 1988), implicating the cadherins as an initial site of extracellular Ca^{++} action. Moreover, freeze-fracture of isolated rat liver membranes, enriched for tight junctions, in the presence of a Ca^{++} chelator show undisturbed strand integrity within the plane of the membrane (Stevenson and Goodenough, 1984). This suggests that other cellular, perhaps cytoskeleton based, Ca^{++}-dependent events are required for modulation of the TJ.

Virtually nothing is known about the function of any of the TJ-associated proteins. It was the intention of this thesis research to help elucidate the role that ZO-1 plays in the regulation of TJ physiology using antisense RNA techniques. The rationale for this approach was based on previously successful antisense approaches to study the function of other membrane-associated (Fernandez et al., 1993) and cytoskeletal proteins (Knecht and Loomis, 1987; Knecht, 1989; Schulze et al., 1989; Liu et al., 1992). Results from these experiments suggested that a technique involving the stable genomic integration of a plasmid vector construct containing an inducible antisense portion of the ZO-1 cDNA into cultured cells may be successful in reducing endogenous ZO-1 protein production. Under the control of an inducible promoter, antisense expression was regulatable and

allowed a contrast of non-induced versus induced cellular states.

Moreover, antisense synthesis could be induced during conditions of stable cell growth in Ca^{++}-containing medium or at critical times of intracellular TJ establishment such as the re-addition of Ca^{++} to cells grown in Ca^{++}-deficient medium. It has been shown that intracellular pools of ZO-1 mRNAs are approximately 10 times more abundant under contact naive conditions prior to the induction of cell-cell contact (Anderson et al., 1989). After Ca^{++}-induced cell-cell contact, the inducible synthesis of antisense RNA theoretically enable the targeting and destruction of ZO-1 mRNA during a critical point in junctional assembly. Immunoblots were used to determine the effects of antisense expression on ZO-1 protein levels, and TER measurements were used to assess the different cellular phenotypes under ZO-1 depleted versus normal conditions to determine whether, by this assay, ZO-1 had a role in TJ assembly.

Materials and Methods

Unless otherwise specified all reagents were purchased from Sigma (St. Louis, MO, USA).

A. Isolation of Canine ZO-1 cDNA

A canine ZO-1 cDNA, designated as dZ3, was confirmed by screening three plaque purified cDNA-containing λ phage, previously identified as expressing segments of the ZO-1 protein by mAb screening (Stevenson, unpublished data), with a portion of the full length rat ZO-1 cDNA, rZ1 (Anderson et al., 1989).

Phage Amplification and λ-dZ3 DNA Isolation

Following the identification of a positive cDNA-containing λ gt11 clone phage, DNA was amplified and isolated. 100 ml of NZCYM medium was inoculated with 100 μl of an overnight culture of strain Y1090 E.coli, grown to an OD_{600} = 0.2-0.3, centrifuged and the pellet was resuspended in sterile 0.01 M $MgSO_4$ to a final OD of 1.0. dZ3-containing λ plaques were picked with a pasture pipette, placed in 1 ml of λ diluent (10 mM Tris-HCl, pH 7.5, 10 mM $MgSO_4$), and eluted for at least 2 hrs at room temperature (RT). Aliquots of 10 μl and 100 μl of phage were added to separate 500 μl aliquots of prepared host bacteria and allowed to preadsorb for 30 (min) at 38°C. Bacteria were added to 37 ml of NZCYM and grown at 38°C, with mild agitation, for 12-15 hrs. A solution containing 100 μl chloroform and 370 μl of nuclease

solution (50 mg DNase, 50 mg RNase A, in 10 ml of 50% glycerol, 30 mM sodium acetate, pH 6.8) was added, and the mixture was incubated at 37°C for 30 min. 2.1 g NaCl was added and mixed until dissolved, and the tube was centrifuged for 20 min at 7,000 rpm (SS-34 rotor, Sorval)at 4°C. The supernatant was combined with 3.7 g PEG 6000-8000 (Baker Scientific, Toronto, Ontario) and placed on ice for 60 min. This was again centrifuged at 7,000 rpm for 20 min at 4°C. The pellet was resuspended in 500 μl of λ diluent. 500 μl of chloroform was added and the mixture was centrifuged at 14,000 x g for 5 min. The supernatant was combined with 20 μl 0.5 M EDTA, 5 μl 20% SDS, and 10 μl 2.5 mg/ml proteinase K (Promega Corp., Madison, WI) and incubated at 65°C for 30 min. This was extracted with 24:1 phenol:chloroform 1-3 times, and once with chloroform. 170 μl of 6 M ammonium acetate was added and the DNA was precipitated with 700 μl of isopropanol and centrifuged for 15 min at 14,000 x g at RT. The pellet was rinsed in 70% ethanol, dried, and resuspended in 500 μl 10 mM Tris-HCl and 1 mM EGTA (TE).

B. Vector Constructs Used for Transfection and Sequencing

λ phage DNA was EcoRI restriction digested and a 1 kb fragment, dZ3, was resolved by gel electrophoresis. dZ3 was subcloned into to the pUC19 plasmid vector (designated pUC19dZ3) and sequenced as described below. dZ3 was then subcloned in the antisense orientation, as confirmed by

restriction analysis, into the pMTX vector (provided by Dr. Colin Rasmussen, University of Alberta) containing the human metallothionien promoter for Zn^{++} inducible expression (designated pMTXdZ3). The pMAMneo cassette (also provided by Dr. Colin Rasmussen, University of Alberta) used to co-transfect with pMTXdZ3 was used as selectable marker.

C. Cell Culture

Madin-Darby canine kidney II (MDCK) cells (low resistance clone N8; Nelson and Veshnock, 1987), a canine kidney epithelial cell line, were grown in Dulbecco's modified Eagle's medium (DMEM; Hazleton Biologics, Lenexa, KA) with 10% fetal calf serum (FCS; Hyclone Laboratories, Logan, UT) 50 U/ml penicillin, 50 μg/ml streptomycin, and 2 mM glutamine. Cells were plated onto 24 mm Transwell permeable cell culture supports (Costar, Cambridge, MA) at 1.4 X 10^6 cells/filter, and grown with daily replenishment of media. Cells were initially plated in normal medium (1.3 mM Ca^{++}) for 90 min and then rinsed 3X with phosphate buffered saline (PBS) without added Ca^{++} or Mg^{++}. Cells were then grown in medium with Ca^{++} lacking from the DMEM formulation containing FCS dialyzed extensively against 0.9% saline (low Ca^{++} medium, LCM). The Ca^{++} concentration in this medium, previously determined by mass spectrophotometry, is ~5 μM (data not shown).

D. Transfections

Prior to transfection, a 15 day survival assay was performed on MDCK cell grown in medium containing increasing G418 (gentamyacin) concentrations; 0, 10, 50, 80, 100, 150 and 200 μM G418 was used. Cells were plated at confluence in T75 culture flasks and maintained for 15 days. During this time cells were fed medium containing fresh G418 once every four days. Cells were then counted.

DNA-$CaPO_4$ co-precipitation was performed by combining 0.5 ml HEPES buffered saline (HBS), 0.1 M $CaCl_2$, pH 7.0 and 20 μg total DNA (5:1 antisense vector:neo cassette, as quantified by optical densitometry). This was mixed for 20 sec and left at room temperature for 30 min. One subconfluent dish (1 x 10^8 cells) of MDCK cells was trypsinized, and the cells were centrifuged at 300 x g for 3 min. Cells were resuspended at a concentration of 0.5-1 x 10^6 cells/ml in 5 ml medium (MEM) supplemented with FCS. One ml of cell suspension was transferred to a 10 cm dish and the entire DNA-Ca^{++} co-precipitate was added with agitation. This mixture was incubated at room temp for 15-20 min. 3.5 ml of MEM medium supplemented with 5% FCS and 200 μM chloroquine was added with agitation. The cells were incubated overnight at 37°C, the medium was removed, and the cells washed once with chloroquine containing MEM medium. 2 ml of HBS containing 15% glycerol were added. The cells were incubated for 60 seconds at 37°C, washed twice with medium,

and grown two to three days in 10 ml of medium to allow several cell divisions.

Cells from both mock transfected dishes, lacking both plasmid vector constructs, and transfected dishes were trypsinized, centrifuged, and resuspended in 10 ml of selection medium (10 ml MEM growth medium/200 μM G418 (as described in results)/10% FCS) and plated. After 20 days G418 resistant colonies were washed twice with PBS and then all liquid was aspirated off. Cloning cylinders (Bellco, Vineland, NJ) were sterilized by flaming in ethanol, placed around each colony and 50 μl of trypsin was added. The colonies were incubated for 10 min at 37°C and subjected to mild trituration to help dislodge the cells. Cells from each colony were transferred to chambers in 96-well dishes, grown to confluence, trypsinized and replated in 24-well dishes. Colonies were grown until 10^7 cells for each colony was achieved. Cells were then maintained as previously described.

E. Southern Blot Analysis

To assess cell transfection, Southern blot analysis was done using both radiolabeled dZ3 or pMAM-Neo cDNAs as probe. 10 μg of DNA isolated from both untransfected and transfected cell lines was digested to completion with EcoRI, BamHI, or HindIII in a final volume of 20 μl. Ethidium bromide-containing loading dye (0.25% bromphenol blue, 0.25% xylene cyanol, 30% glycerol) was added and

samples were loaded onto a 1% agarose (FMC, Rockland, ME) gel and electrophoresed. The gel was placed in a solution of 0.2 N HCl for 10 min and in denaturation solution (1.5 N NaCl, 0.5 N NaOH) for 20 min. The DNA was transferred by capillary action from the gel to a nylon membrane (Schleicher and Schuell, Keene, NH) overnight. The membrane was removed, placed in a UV Stratalinker (Fisher Scientific, Pittsburgh, PA), and exposed to 1200 J of ultraviolet radiation. The blot was placed in a prehybridization solution of either Westneat (7% SDS, 0.26 N $NaPO_4$, 5x Denhardts (0.1% Ficoll, 0.1% polyvinylpyrrolidone, 0.1% bovine serum albumin), 0.01 N EDTA) and incubated at 65°C overnight or Rapid Hybe (Amersham, Arlington Heights, IL) for 2 hours. cDNA probes were radiolabeled with ^{32}P-αdCTP (NEN, Mississauga, OT) using the Prime-it Random Primer Labeling Kit (Stratagene, La Jolla, CA) and unincorporated nucleotides were removed by passing the reaction mixture through a NucTrap probe purification column (Stratagene). An aliquot of purified probe was quantified for radionucleotide activity using a beta counter (Fisher). Specific activities ranged between 5-10 $x10^7$ cpm/ul. Probe was added to the prehybridization mixture and the blot was incubated at 65°C overnight. The blot was washed twice with 0.5 x SSC (0.0075 M sodium citrate and 0.075M sodium chloride), 1% SDS (sodium dodecyl sulphate) at 42°C and twice with 0.05 x SSC, 1% SDS 55°C and exposed to film for 24 to 96 hours.

Southern blot analysis used to determine copy number sensitivity was done as above with the following modifications. pUC19dZ3 DNA was quantified using a spectrophotometer and EcoRI restriction-digested to completion. Agarose gel lanes were loaded with DNA equivalent to one, five, twenty-five, and fifty dZ3 insert copies/haploid canine genome. The blot was probed with radio-labelled dZ3 cDNA.

F. Induction of Antisense dz3 RNA Synthesis

Prior to induction a Zn^{++} tolerance experiment was performed on MDCK cells. Cells were grown for 24 hours in media containing 300, 400, 500, 600, or 700 μM Zn^{++} and counted.

Untransfected MDCK and transfected MDCK cells (designated as A1) were plated at confluence on multiple sets of filters and grown for 72 hours in LCM. Half of each type were fed with Ca^{++}-containing medium and the other half fed medium with 1.8 mM Ca^{++} and 300 μM Zn^{++}. TER measurements were taken at 12 or 24 hour intervals for up to 120 hours.

G. Transepithelial Resistance Measurements

TER was determined using a Millicell-ERS apparatus (Millipore Corporation, Bedford, MA). Electrodes were equilibrated in 10 mM HEPES pH 7.4, 5.4 mM KCl, 137 mM NaCl, 1.3 mM $CaCl_2$, 0.5 mM $MgCl_2$, 5.6 mM glucose (HBSG) for 24 hrs prior to experiments. TER measurements were made at RT, and

TER of blank collagen-coated filters was subtracted from all samples.

H. Isolation of Total mRNA

1. Guanidinium isothiocyanate method

Total RNA was isolated from cultured MDCK cells by a modified procedure of Ausubel et al., (1993). A pellet of approximately 1-2 x 10^7 MDCK cells was resuspended in 1 ml of denaturation solution (4 M guanidinium thiocyanate, 25 mM sodium citrate, pH 7.0, 0.1 M 2-mercaptoethanol, 0.5% N-laurosarcosine). This was made 0.1 M in sodium acetate. 1 ml water-saturated phenol and 400 µl of 49:1 chloroform/isoamyl alcohol was added, mixed, and incubated at 4°C for 20 min. This mixture was centrifuged at 14,000 x g for 15 min at 4°C and the upper aqueous phase was removed and transferred to a fresh tube. RNA was precipitated by adding 1.6 ml of 100% isopropanol and centrifuging at 14,000 g for 15 min at room temp. The pellet was redissolved in 100 µl of denaturation solution, reprecipitated and disolved in 100 µl distilled water. The isolation of total RNA was also accomplished using TRIzol Reagent (Gibco) according to the protocol of Chomczynski and Sacchi, (1987). In brief, a monophasic solution of phenol and guanidinium isothiocyanate was used to solubilize an MDCK cell pellet. Chloroform was added, mixed, and centrifuged. The RNA-containing aqueous phase was precipitated with isopropanol.

I. Northern Blotting

RNA was quantified by absorbance at 260 nm, and 5-10 μg of total RNA was mixed with 15 μl of loading buffer (1.3 x MOPS, 6.7% formaldehyde, 65% formamide). RNA samples were heated at 68°C for 10 min, briefly centrifuged, and loading dye was added. These samples were electrophoresed through a denaturing gel (1% agarose, 1 x MOPS, 2.5% formaldehyde) in running buffer (2.5% formaldehyde, 1 x MOPS) at 65-80 volts. The gel was then washed in 10 x SSC for 45 min.
Immobilization of RNA on a nylon filter was achieved through overnight capillary transfer. The nylon membrane was pre-wet in distilled water for 5 min and 20 x SSC for 10 min. Filter paper was pre-wet in 20 x SSC. Following transfer, the nitrocellulose was rinsed for 10 min in 6 x SSC and RNA was bound to the membrane by a 1200 J burst of ultraviolet irradiation. The membrane was placed in a solution of prehybridization buffer [5 x Denhardts, 5 x PIPES (piperazine-N,N'-bis[2-ethanesulfonic acid]), ± 50% formamide, 1% SDS, 500 μg/ml salmon sperm DNA) for 2-16 hours at 37°C with formamide-containing prehybridization solution or at 65°C without formamide. Blots were then washed with varying stringencies: twice in 2 x SCC, 1% SDS at room temperature, twice in 0.5 x SSC, 1% SDS at 42°C for total MDCK RNA probed with rZ1 cDNA; twice in 0.5 x SSC, 1% SDS at RT, twice in 0.05 x SSC, 1% SDS at 55°C for total

MDCK RNA probed with dZ3. cDNA probes were prepared and added as previously described.

J. Quantitative Western Blotting

Protein isolated from transfected and untransfected cell lines was quantified and the linearity of response was assessed according to the method of Stevenson et al., (1994) using ^{125}I-biotin/streptavidin reagents.

K. PCR

The second canine ZO-1 cDNA, dZ4, was isolated by the polymerase chain reaction (PCR). To create cDNAs for PCR (Kleppe et al., 1971; Saiki et al., 1986) 5 μg of total RNA isolated from MDCK cells was heated at 90°C for 5 min, chilled on ice, and added to a reverse transcriptase reaction mixture (50 mM KCl, 20 mM Tris-HCl 2.5 mM $MgCl_2$, 100 μg/ml bovine serum albumin, 0.25 mM dATP, 0.25 mM dCTP, 0.25 mM dGTP, 0.25 mM dTTP, 20 U RNasin, 100 pmol random hexamer). 20 U of MoMuLV reverse transcriptase (Promega) was added and the mixture was incubated for 10 min at 23°C, 60 min at 42°C, 5 min at 95°C and quick chilled on ice for 2 min. This mixture was extracted once with buffered phenol and once with 24:1 chlorophorm:isoamyl alcohol. cDNA was precipitated with 0.3 M sodium acetate and an equal volume of 100% ethanol, centrifuged at 14,000 x g and resuspended in 40 μl water. To amplify dZ4 cDNA, 5 μl of the cDNA was added to a mixture containing 50 mM KCl, 20 mM Tris-HCl, 2.5 mM $MgCl_2$, 100 μg/ul bovine serum albumin, 0.25 mM dATP, 0.25

mM dCTP, 0.25 mM dGTP, 0.25 mM dTTP, 25 pmol of each primer, and 2 U of Taq polymerase (Promega). The upstream (5′) primer was 5′-GGGATCCAGATGTGGATTTACC-3′ and the downstream (3′) primer was 5′-GGAATTCCAGGGGAGTCTATTC-3′. The downstream primer was created by comparing the 5′ dZ3 terminus with the incomplete human sequence and the upstream primer by selecting a site of least degeneracy 1500 base pairs further up the human ZO-1 sequence.

L. Sequencing

The full length sequence of dZ3 and the partial sequence of dZ4 were obtained by sequencing techniques which were modified forms of the dideoxy chain termination method (Sanger et al., 1977 and 1980). The terminal 5′ and 3′ 250 base pairs were sequenced using the US Biochemical, Sequenase Kit, version 2.0 (Tabor and Richardson, 1990). Sequencing of the rest of the dZ3 clone and the 5′ and 3′ terminal 200 base pairs of the dZ4 clone was done by a fluorochrome-coupled dideoxy nucleotide chain termination technique (Core Sequencing Facility, Department of Biochemistry, University of Alberta). The sequence of dZ3 was bi-directionally extended by designing primers based on successive sequence information. Four oligonucleotide primers for each strand were created and utilized to derive overlapping sequence information which was aligned and made contiguous.

Results

A. Isolating Canine Specific ZO-1 cDNAs

A 1017 base pair fragment of the previously identified rat ZO-1 cDNA (rZ1, Anderson et al., 1989), was used as a probe to identify a canine ZO-1 cDNA. One of three plaque purified λ gt11 clones, previously isolated by immunoscreening of a canine brain expression library with a cocktail of anti-ZO-1 mAbs (Fig. 1a), was positively identified by hybridization (Fig. 1b). The insert was excised from the λ vector by restriction enzyme digestion with EcoRI and was characterized by agarose gel electrophoresis as a fragment of approximately 1 kb (Fig. 1c). Northern blot analysis of MDCK total mRNA probed with the 1 kb insert identified a 7.5 kb transcript (Fig. 2) corresponding to the expected size of the ZO-1 message (Anderson et al., 1989). The cDNA was subcloned into the pUC19 plasmid vector and bi-directionally sequenced (Fig. 3a). The 5′ terminal was aligned with partial rat, canine, and human sequences. At the nucleotide level this cDNA showed 83.8% identity with the human ZO-1 sequence (Willot et al., 1993), 91.6% identity with the mouse ZO-1 sequence (Itoh et al., 1993), and 98.1% identity with a partial rat ZO-1 cDNA, rZ1 (Anderson et al., 1989), confirming that it was the canine ZO-1 equivalent. Conceptual translation of the open reading frame (ORF) encoded by dZ3 could be

positioned in relation to the human ZO-1 sequence (Fig. 4). Internal primer positions and sequencing strategy are also shown.

To extend the canine ZO-1 sequence, two 17 bp opposing degenerate oligonucleotide primers were created which spanned 1500 bp upstream of dZ3 according to the human sequence. In RT-PCR reactions involving both canine RNAs these primers were able to resolved a single 1.5 kb product on an agarose gel (Fig. 5a). A single high molecular weight band at the ZO-1 position was detectable using the canine-derived PCR products as probes in Northern blots of canine total RNAs (Fig. 5b). This PCR product was partially sequenced using the initial degenerate oligonucleotides as sequencing primers. Sequence derived from the 5' terminus showed 88% sequence identity, at the nucleotide level, to the human sequence (Fig. 6), confirming it as a portion of the canine ZO-1 cDNA. This sequence was designated as dZ4 and subcloned into the pUC19 plasmid vector.

B. Constructing Antisense Expressing Cell Lines

Prior to transfection, a G418 dose response survival assay was performed to determine what concentration was needed to kill all untransfected cells within 15 days. Results show that 200 μM was sufficient (Fig. 7). The dZ3 fragment was excised from the pUC19 vector and subcloned in both sense and antisense orientations into the EcoRI site of

the pMTX plasmid vector (Fig. 8a). Orientations were confirmed by EcoRI and PstI restriction digestions of sites determined from initial sequence information. The antisense construct, under the control of the metallothionien inducible promoter, was co-transfected with the pMAMneo plasmid vector (Fig. 8b) into MDCK cells. Mock transfected MDCK cells, which lacked only plasmid vector constructs from the transfection protocol, did not produce any G418 resistant colonies. Five G418 resistant colonies were isolated from transfected dishes, and designated A1, A2, A3, A4, and A5. Only A1 was used in the TER and protein level studies described hereafter.

C. Verification of Genomic pMTX-dZ3

Clone A1 demonstrated multiple pMTXdZ3 genomic integration sites as indicated by Southern blot analysis using dZ3 cDNA as probe (Fig. 9). Southern blots using genomic DNA isolated from untransfected MDCK cells as control, again probed with dZ3 cDNA, resolved neither the multiple banding pattern observed in the clonal line nor any other bands. These results indicated that there was DNA present in the A1 clonal line which was foreign to the untransfected MDCK cells. More importantly, a 1 kb EcoRI fragment is identified as expected if pMTXdZ3 is stably integrated into the A1 genome (Fig. 9 lane 3). However, the inability of Southern blots to identify fragment(s) common

to either cell line, corresponding to the endogenous ZO-1 gene, indicated that the sensitivity of the Southern blot was low and could not resolve a genomic ZO-1 gene in single copy but could identify multiple copies and integrations of dZ3 sequence. To assess whether the Southern blot sensitivity was too low to identify a single copy gene, single to multiple copies of dZ3 insert were blotted and probed with dZ3 cDNA to determine the limits of Southern blot sensitivity. The results indicated that identification of the dZ3 insert under these conditions was possible at copy number five (Fig. 10); however, there was no visible band at a single copy. This indicated that the genomic ZO-1 gene is undetectable in single copy by these Southern blot techniques.

Northern blot analysis, using radiolabelled dZ3 as probe, could not detect the presence of an antisense transcript 4, 12, or 16 hours after Zn++ induction although the ZO-1 message could be detected (data not shown).

D. Transepithelial Resistance and ZO-1 Protein Levels

Given that the tight junctional barrier is responsible for the regulated movement of ions through the paracellular pathway, resistance measurements derived from a current passed across a filter-plated cell monolayer is a reasonable measure of tight junctional permeability in most circumstances. The effects of antisense ZO-1 RNA production

on tight junction physiology was tested by this assay. Assays on TER development and correlative ZO-1 protein levels were done using a calcium switch paradigm in which cells, after living in LCM for 72 hours, were switched to Ca^{++}-containing medium with or without Zn^{++}(to induce antisense ZO-1 RNA synthesis) and grown and characterized for several days. A dose-response experiment showed that MDCK cells at confluence under physiologic Ca^{++} conditions were able to tolerate up to 500 μM Zn^{++} before survival was affected (Fig. 11). Accordingly, a concentration of 300 μM Zn^{++} was selected for induction experiments on the transfected MDCK cells, clone A1. Two different results were consistently obtained after Zn^{++}-induction in the Ca^{++}-switch assay. The results of several experiments indicated that after the addition of Ca^{++} and Zn^{++} there was a significant delay in TER development in the A1 cells relative to controls (Fig. 12). Although transfected A1 cells in the absence of Zn^{++} also demonstrated a lag in TER development, Zn^{++}-induced A1 cells consistently showed a longer delay. Untransfected cell lines showed a faster rise in TER than either the Zn^{++}-treated or Zn^{++}-untreated A1 cell lines. The Zn^{++}-induced delay was reversible as A1 cells developed a normal TER after the removal of Zn^{++} from medium (Fig. 13), indicating that cell death was not the cause of slower TER development. In a separate experiment, Zn^{++}-induced A1 cells which showed low TER values after 48 hours (Fig. 14a) were

harvested, along with the control-treated cells, for total protein. Quantitative western blots loaded for equivalent protein (using the BCA method) showed ZO-1 levels in Zn^{++}-induced A1 cells to be markedly lower than those of controls (Fig. 14b) ^{125}I quantification of the immunoblot data indicated that there is less ZO-1 in the low TER cells (Fig. 14c). All ^{125}I values were interpreted in the linear range (Fig. 14d). This type of result was, however, contrasted by those obtained from other experiments which showed TER values of Zn^{++}-induced A1 cells to develop more rapidly and to a greater value than the TER of controls. TER values obtained from Zn^{++}-treated A1 cells relative to control-treated cells were almost 3 fold higher after 24 hours (Fig. 15a). Corresponding protein isolated from the control as well the A1 cells under these conditions indicated that there was an increased ZO-1 protein content in the A1 cells relative to the controls (Fig. 15b). ^{125}I quantification of ZO-1 levels confirms more ZO-1 in the high resistance cells (Fig. 15c).

Discussion

To assess the role of ZO-1 in the function of the TJ, a canine ZO-1 cDNA, dZ3, was isolated by hybridization screening with a rat homolog, rZ1. dZ3 was sequenced and subcloned, in the antisense orientation, into the pMTX plasmid vector construct containing the metallothionien promoter for Zn^{++}-regulated expression. Using the Ca^{++}-switch tight junction assembly paradigm, transfected cell monolayers were concurrently exposed to Ca^{++} and Zn^{++}. The effects of Zn^{++}-induced antisense dZ3 RNA synthesis were assessed by ZO-1 protein quantification and measurements of TER development. Two widely different sets of results were obtained. In the first case, transfected cells exposed to Zn^{++} showed a significant lag in TER development and an associated decrease of ZO-1 protein relative to controls. In the second case, transfected cell monolayer TER values were dramatically increased and ZO-1 protein levels were much higher relative to controls following Zn^{++} exposure.

There is no direct evidence which implicates ZO-1 as part of the regulatory scheme of the TJ. Confluent MDCK cells grown in medium containing physiologic levels of Ca^{++}, show a TJ-associated form of ZO-1 which has a significantly higher phosphate content than the cytoplasmically distributed ZO-1 of MDCK cells grown in low Ca^{++}. These results which indicate that ZO-1 phosphorylation is

regulated under certain conditions, perhaps is related to the intracellular distribution of ZO-1 (Howarth et al., 1994). It has been shown, by TER measurements and immunofluorescence, that protein kinase inhibitors can retard the disassembly of the TJ and ZO-1 re-distribution upon calcium depletion (Citi, 1992) as well as TJ assembly and ZO-1 recruitment upon Ca^{++} re-addition (Nigam et al., 1991). This would suggest that phosphorylation of a component(s) in the Ca^{++} stimulated pathway is important in TJ assembly/disassembly. Acute removal of Ca^{++}, however, has not been shown to alter the distribution (within 5 min) or the phosphate content of ZO-1, indicating that ZO-1 is probably not an immediate target of the aforementioned protein kinases in junctional assembly/disassembly, at least within the resolution of these experiments. On the other hand, results shown here of both TER and protein quantification indicate that there is a positive correlation between ZO-1 protein levels and the development of TER in the MDCK cell line. This is the first evidence of a direct role for a TJ-associated protein in the assembly of the TJ.

Two widely discrepant results were obtained in Ca^{++}-switch experiments. In the first case, TER and ZO-1 protein levels of Zn^{++}-treated A1 cells are lower than controls. A consistent lag in TER development in A1 cells which were not exposed to Zn^{++} indicates that there may be leakiness of the hMTIIa metallothionien promoter causing low level

constitutive synthesis of antisense ZO-1 mRNA leading to decreased ZO-1 protein levels. Nonetheless, Zn^{++}-treated A1 cells show a more dramatic lag in TER development and associated lack of ZO-1 protein. Other results demonstrate a marked increase in the rate of TER development and associated ZO-1 protein synthesis following Zn^{++} induction of A1 cells. Though these opposing effects have been shown after Zn^{++} induction, there remains an imprecise positive correlation between TER values and ZO-1 protein content. Undoubtably there are other variables which effect TJ permeability. ZO-1 protein content is unlikely to be solely responsible for TER development in MDCK cells. Since both TER and ZO-1 protein values obtained from the Zn^{++}-induced A1 cells were clearly different from other controls, this argues that the coincidental rise or fall of TER/ZO-1 protein levels was a consequence of antisense ZO-1 expression. Depression of A1 ZO-1 protein synthesis and TER development are expected consequences of Zn^{++}-induced antisense expression. However, the increase in ZO-1 protein amounts and TER values in the Zn^{++}-treated A1 cells of other experiments were not anticipated. Explanations for the rise in ZO-1 protein levels may involve the age of the clonal line, as reflected by the number of cell passages. Rapid increases in TER occurred in A1 cells of higher passage number (>4) and was never observed in cells passaged only once or twice, where a consistent delay in TER development

upon Zn^{++} induction was observed. The antisense dZ3 RNA expression of higher passage number A1 clones may have been suppressed and even compensated for by over-expression of endogenous ZO-1 mRNA, as indicated by the high ZO-1 protein levels shown in figure 16. Precedents for this bypass of stable antisense inhibition exist and show a correlation with higher passage number. Antisense approaches to the elimination of myosin heavy chain (Knecht, 1989) and α-actinin (Schulze et al., 1989) have shown the anomalous re-expression or overexpression of the antisense target protein. The relationship between protein and antisense RNA levels is complex. In some studies it has been shown that less protein was detected without an observable decrease in the amount of sense mRNA (Knecht 1989). Moreover, protein re-expression has been shown to occur even in the presence of abundant antisense transcript (Fernandez et al., 1993). The presence of an RNA duplex unwindase activity (Bass and Weintraub, 1987) or the formation of secondary antisense RNA structures (Liu et al., 1992) may have also been reasons for the inability of the antisense transcript to eliminate ZO-1 protein function in some experiments.

It is important to note that the 1 kb antisense dZ3 transcript could not be detected by Northern blot analysis. The explanation may lie in the inability of this assay to detect only stable RNA in the cell. If hybrid formation takes place in the nucleus, then the steady state level of

RNA in the nucleus is the critical parameter driving hybrid formation. A Northern blot measures the steady state level of RNA in the cytoplasm. With a heterologous gene fusion construct such as pMTXdZ3, the transcription rate, processing time and half life of an antisense RNA are likely to be unpredictable. A nuclear run-on assay might provide a more accurate indication of the antisense dZ3 transcription. Decreases in cellular ZO-1 protein following induction of early passaged A1 cells indicates that induction is correlated to depressed ZO-1 protein synthesis even though an antisense message is undetectable by Northern blot. This result is further supported by the work of van der Krol et al. (1988) who have shown that maximal depression of the chalcone synthase protein in transgenic plants was not correlated with a detectable level of antisense gene expression.

It is unclear how ZO-1 might be involved in the assembly of the TJ at the molecular level. ZO-1 has been shown by immunofluorescent light microscopy to co-localize with actin filaments under a variety of conditions including the co-localization of ZO-1 and actin aggregates in cytochalasin D-treated cells (Stevenson and Begg, in press). ZO-1 has also been shown to localize to the actin dense lamellipodia of S180 cells in the absence of cell-cell contact (Howarth et al., 1993) and at adherens junctions of heart intercalated disks, a site of actin-membrane

interactions (Itoh *et al.*, 1991). In addition ZO-1 has been shown to bind spectrin (Itoh *et al.*, 1993). These data suggest that ZO-1 may be involved in mediating actin-membrane interactions. Like other junctional complexes the formation of a junctional "plaque" comprised of many proteins peripherally associated with the membrane precedes and nucleates the establishment of a cytoskeletal connection to the membrane. Madara (1987) observed that actin filaments interacted with a "plaque" of material immediately adjacent to the points of membrane contact at the tight junction. Although the composition of this plaque is unresolved, ZO-1 is localized by immunoelectron microscopy to the same sites (Stevenson *et al.*, 1989), suggesting that ZO-1 may be part of this structure. Preventing the recruitment of ZO-1 to this plaque during its formation may hinder the formation of a stable junctional complex and create a leaky TJ.

ZO-1 shows 47% identity at the nucleotide level to the *dlg* gene of *Drosophila*. Mutations in dlg caused apical-basolateral depolarization and the loss of intercellular adhesion of epithelial cells within imaginal discs. Other mutations in *dlg* caused neoplastic growth. These results implicate *dlg* in a signal transduction pathway responsible for controlling proliferation in mitotically active tissue. The mechanism whereby this is facilitated may involve the *src* oncogene homology (SH3) and/or the guanylate kinase (GK) like domains which are common to both *dlg* and ZO-1.

Accumulating evidence suggests that SH3 domains bind to a variety of proteins that regulate the activity of small GTP-binding proteins by controlling the ratio of bound GTP to GDP. The observation that the small GTPase, Rab 13, has been shown to co-localize with ZO-1, creates the possibility that ZO-1 may act as a signal transducer to control the activity of Rab 13. ZO-1 in this capacity may therefore act as a signal transducer to control the chemical state of other plaque proteins. Depletion of ZO-1 may result in the disruption of a signalling cascade responsible for the tightness of the TJ.

Further examination of the specific domains of ZO-1 are necessary to elucidate the role various regions of the ZO-1 molecule play in regulating the permeability of the TJ. Over-expression of the full length ZO-1 and cDNA as well as portions of the protein such as those encoding the α, SH3, and GK domains may provide evidence for their specific roles. Expression of certain cDNA regions may show dominant negative effects and elucidate the importance of certain regions within ZO-1.

Figure 1. Plaque purified ZO-1 clone isolated from canine λ cDNA expression library. a) nitrocellulose lift of induced β-gal fusion protein probed with anti-ZO-1 mAbs and visualized by peroxidase conjugated secondary antibodies. b) autoradiograph of similar lift probed with ^{32}P-labelled 1 kb rat ZO-1 cDNA, rZ1. c) Agarose gel of EcoRI digested phage DNA showing a 1 kb insert, lane 1, and DNA standards, lane 2.

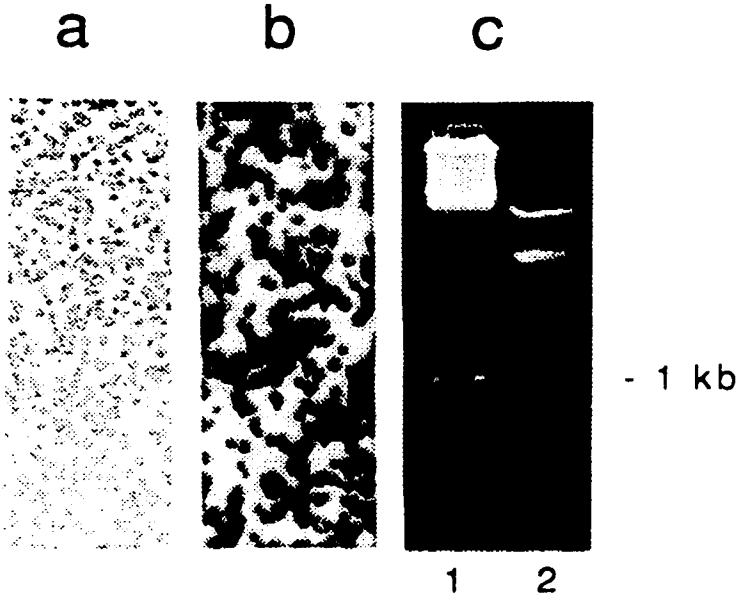
a
b
c
- 1 kb
1
2

Figure 2. Northern blot analysis of total RNA from MDCK cells hybridized with the 1 kb insert (dZ3) shown in figure 1c, lane 1 labelled with ^{32}P. ZO-1 mRNA migrates at approximately 7.5 kb. The positions of 28 S and 18 S rRNAs are indicated.

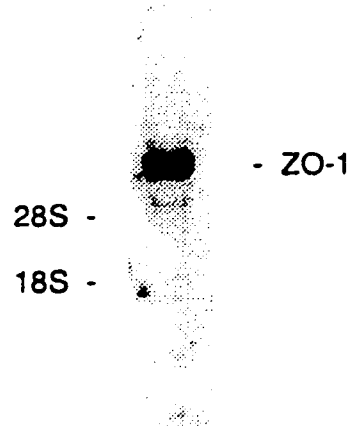
- ZO-1
28S -
18S -

Figure 3. a) Complete sequence of the partial canine ZO-1 cDNA, dZ3. b) An alignment of the 5′ terminus of dZ3 to rat (rZ1), mouse (mouse ZO-1), and human (humzo1orf) ZO-1 cDNAs. dZ3 is 98% identical to the rat ZO-1 cDNA, rZ1, 92% identical to mouse ZO-1 (Itoh et al., 1993), and 84% identical to human ZO-1 (Willot et al., 1993).

a

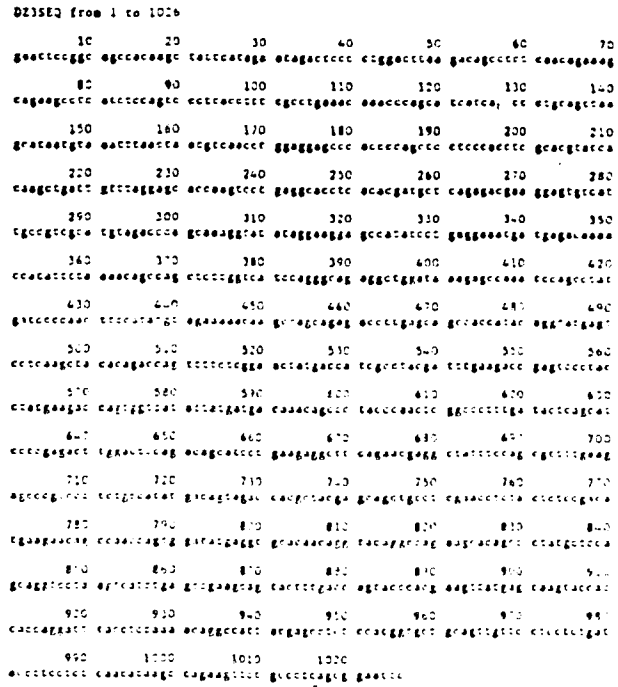

b

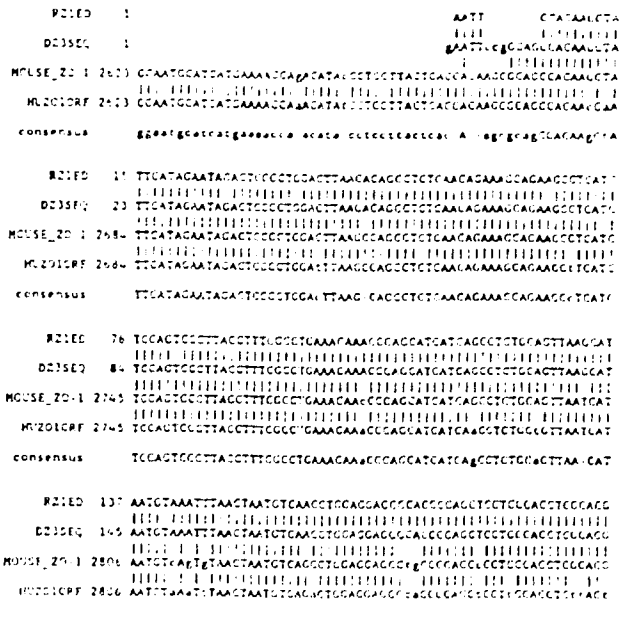

Figure 4. Schematic representation of the position of dZ3 relative to the structural domains within the human ZO-1 cDNA sequence (Willot et al., 1993). Repeat domains of unknown function are labeled 1,2, and 3. SH3, guanylate kinase homology, acidic (+), alternatively spliced (α) and proline-rich domains are also identified. dZ3 spans nucleotides 3899-4910 of the human ZO-1 sequence, which includes α domain (3954-4194). Arrows indicate strategy used to obtain the overlapping bi-directional sequence of dZ3.

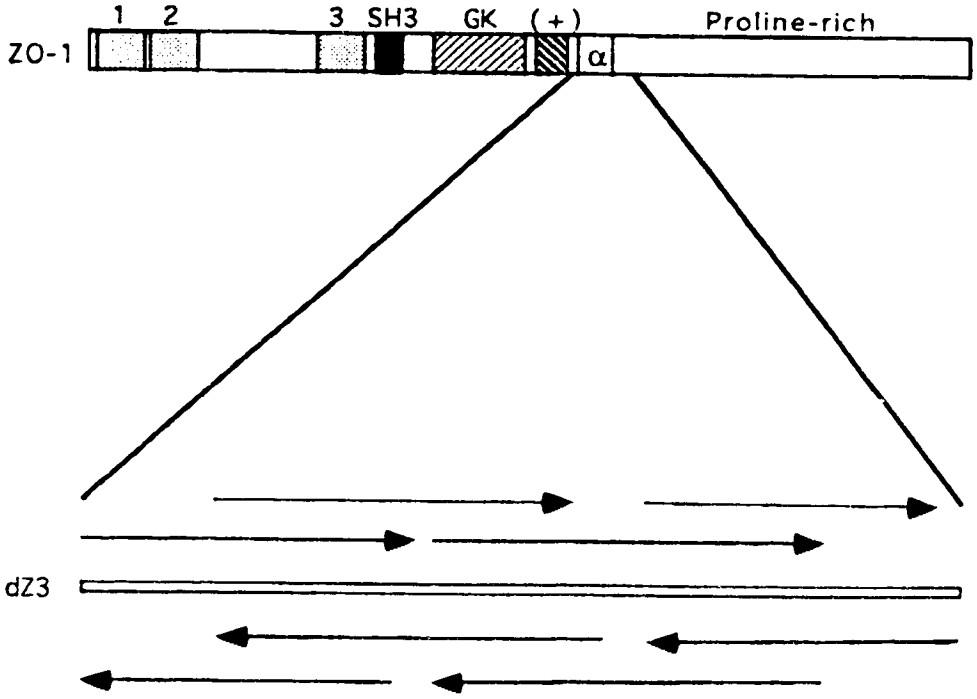
1
2
3
SH3
GK
(+)
Proline-rich
ZO-1
α
dZ3

Figure 5. Characterization of the PCR-derived 1.5 kb cDNA clone of canine ZO-1, dZ4. a) RT-PCR products obtained from MDCK cell total RNA sequences. Products from 6 separate PCR reactions were electrophoresed on a 1% agarose gel. DNA standard of 1636 and 1018 base pairs (lane M) flank the 1500 base pair fragments obtained using primers generated from dZ3 (3′) and human ZO-1 sequences (5′). b) Autoradiograph of northern blot analysis of total RNA from MDCK cells hybridized with the ^{32}P-labelled dZ4 cDNA obtained from PCR. ZO-1 migrates at approximately 7.5 Kb. 28 S and 18 S rRNAs are indicated.

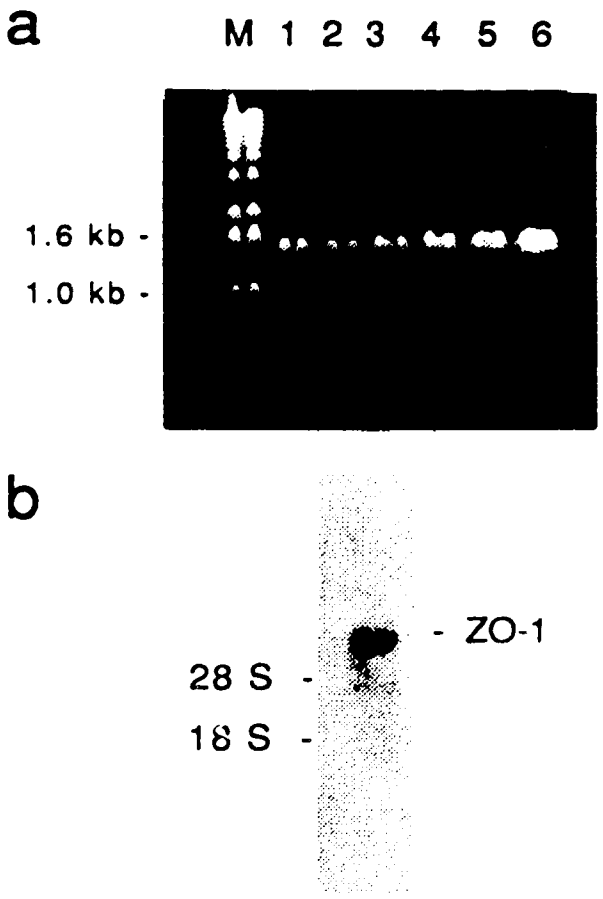
a
M 1 2 3 4 5 6
1.6 kb -
1.0 kb -
b
- ZO-1
28 S -
18 S -

Figure 6. Partial dZ4 cDNA sequence, from the 3′ terminus, compared to the human ZO-1 sequence indicates 88% identity at the nucleotide level.

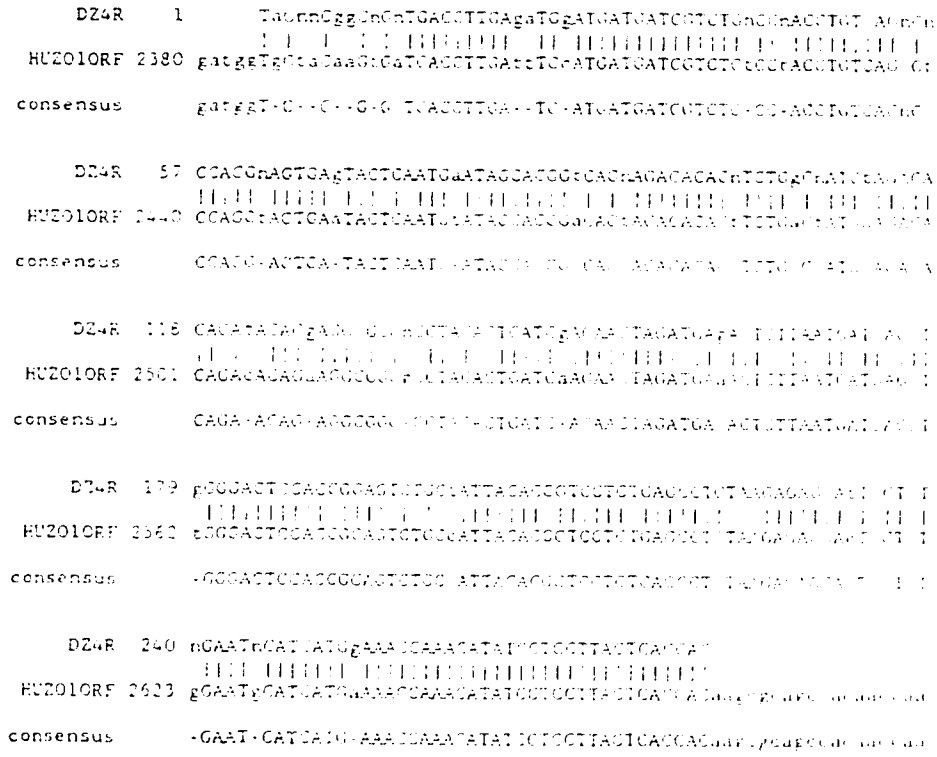

Figure 7. Fifteen day survival assay of cultured MDCK cells grown in G418-containing medium. The effects of increasing concentrations of G418 are plotted against survival, which is expressed as a percentage of surviving control cells not exposed to G418 after 15 days. 200 μM G418 kills all cells after 15 days.

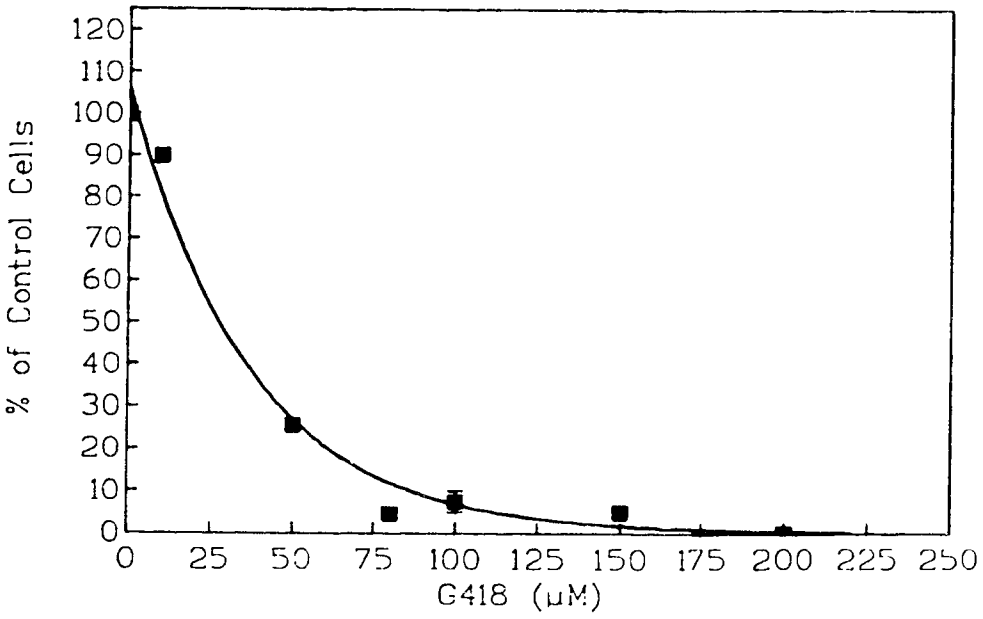
% of Control Cells
120
110
100
90
80
70
60
50
40
30
20
10
0
0
25
50
75
100
125
150
175
200
225
250
G418 (μM)

Figure 8. Vectors used for antisense transfection and selection. a) Schematic representation of the pMTX plasmid vector construct used to express antisense dZ3. Salient features include the hMTIIa Zn^{++}-responsive upstream regulatory element used to drive transcription, the unique EcoRI restriction site used to subclone dZ3, and the parvalbumin 3′ untranslated (PV 3′ UTR) region used to polyadenylate the antisense RNA. b) Schematic representation of the pMAMneo plasmid vector co-transfected with pMTX. Features include the rous sarcoma virus and mouse mammary tumor virus long terminal repeats (MMTV-LTR) enhancer elements. The simian virus 40 (SV40) early promoter region is used to constitutively drive synthesis of the aminoglycoside acetyltransferase gene which confers G418 resistance.

a

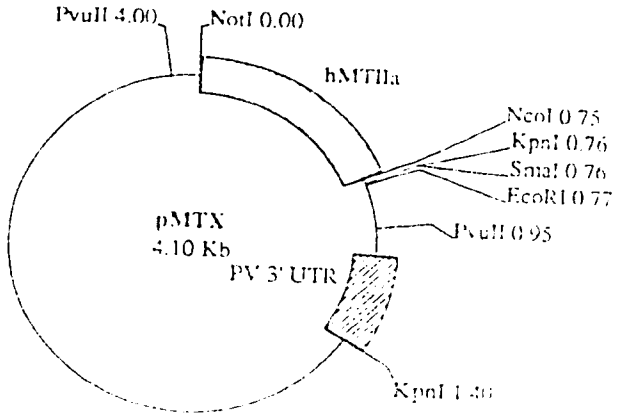
PvuII 4.00
NotI 0.00
hMTIIa
NcoI 0.75
KpnI 0.76
SmaI 0.76
EcoRI 0.77
PvuII 0.95
pMTX
4.10 Kb
PV 3' UTR
KpnI 1.46

b

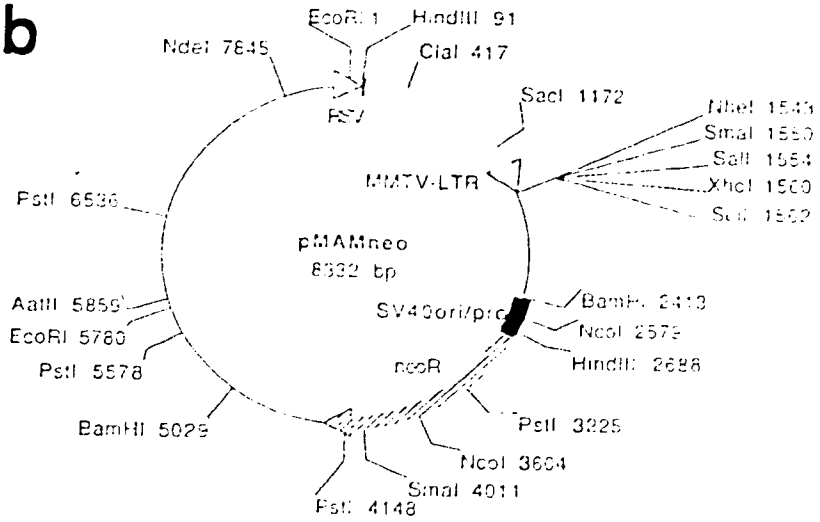
EcoRI 1
HindIII 91
NdeI 7645
ClaI 417
SacI 1172
RSV
MMTV-LTR
PstI 6536
pMAMneo
8332 bp
AatII 5859
EcoRI 5780
PstI 5578
BamHI 5029
SV40ori/prom
BamHI 2413
NcoI 2575
HindIII 2686
neoR
PstI 3825
NcoI 3604
SmaI 4011
PstI 4148

Figure 9. Southern blot analysis of Bam HI, Eco RI, or Hind III restriction endonuclease-digested transfected (T) and untransfected (U) MDCK cell genomic DNA hybridized with ^{32}P-labelled dZ3 cDNA. Intense banding is observed in the transfected lanes, however, no bands are detectable in the untransfected lanes. A 1 kp band is detected, as expected, in the EcoRI digest of transfected cells.

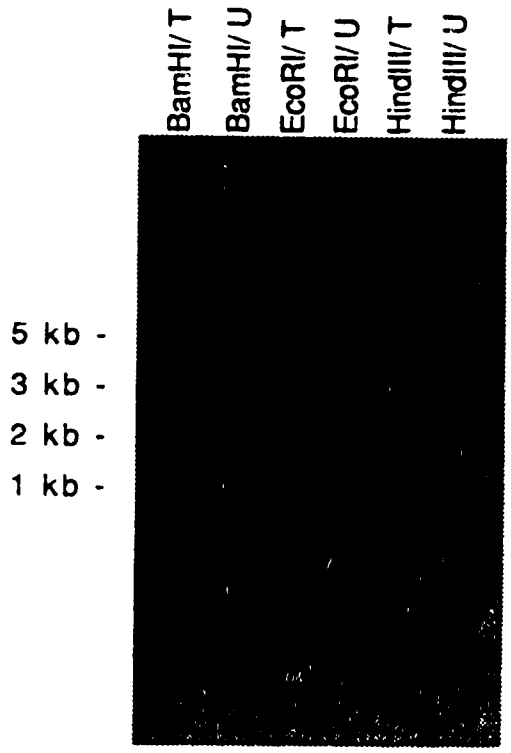
BamHI/ T
BamHI/ U
EcoRI/ T
EcoRI/ U
HindIII/ T
HindIII/ U
5 kb -
3 kb -
2 kb -
1 kb -

Figure 10. Southern blot analysis of 1, 5, 25 and 50 copies of dZ3 insert hybridized with ^{32}P-labelled dZ3 cDNA. A detectable band is first observed at 5 copies.


1 5 25 50

Figure 11. 24 hour survival assay of confluent MDCK cells exposed to increasing Zn^{++} concentrations. Increasing Zn^{++} concentrations are plotted against survival, expressed as relative to the survival of control cells not exposed to Zn^{++}. Survival is noticeably affected at concentrations greater than 500 μM.

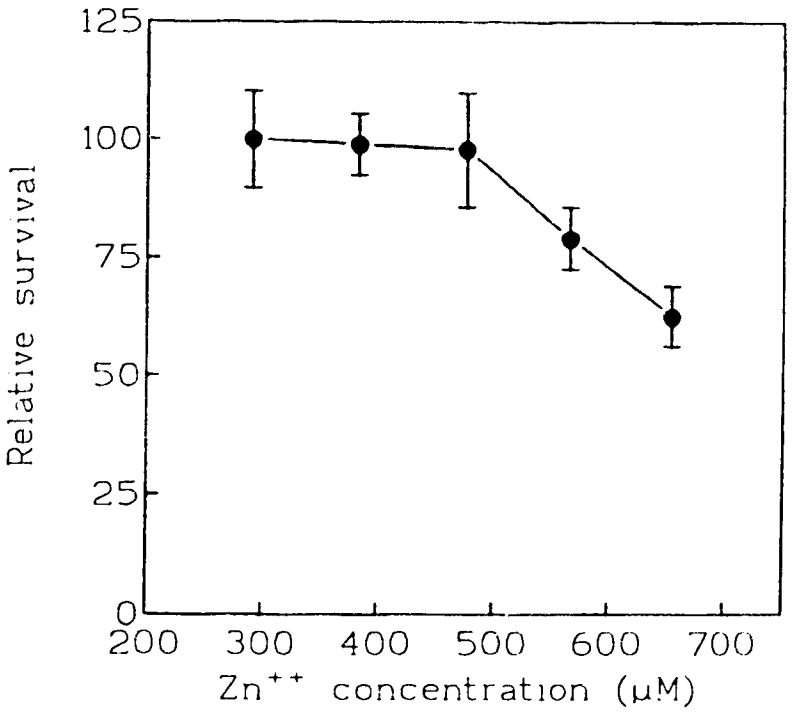
125
100
75
50
25
0
Relative survival
200
300
400
500
600
700
Zn++ concentration (μM)

Figure 12. TER development in transfected versus untransfected cell lines following Zn^{++} induction. Both untransfected and transfected cells were plated on permeable filter substrates and maintained in low calcium (~5 μM) for 3 days. Cells were then switched to medium containing normal levels of Ca^{++} (1.8 mM) to induce the formation of tight junctions. Half the filters from each cell type were exposed to 300 μM Zn^{++} for 72 hours in order to induce the synthesis of antisense ZO-1 mRNA in the transfected line. The development of TER was monitored for 72 hours after switching to normal Ca^{++}. As shown, the parental lines developed normal TER in 12-24 hours in the presence and absence of Zn^{++}. The transfected line grown in the absence of Zn^{++} appears to develop normal TER more slowly than the untransfected line. Interestingly, however, the development of TER in the transfected lines is further delayed by the presence of Zn^{++}, suggesting that expression of antisense ZO-1 RNA and subsequent reduction of ZO-1 protein levels retards tight junction formation.

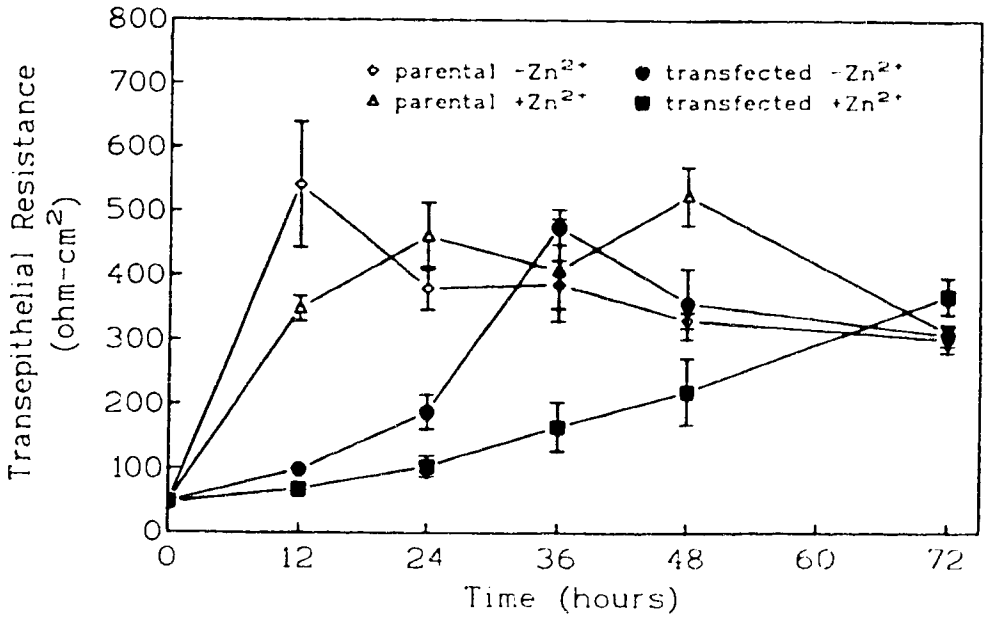
800
700
600
500
400
300
200
100
0
0
12
24
36
48
60
72
Transepithelial Resistance (ohm-cm²)
Time (hours)
parental -Zn²⁺
parental +Zn²⁺
transfected -Zn²⁺
transfected +Zn²⁺

Figure 13. Removal of Zn^{++} allows recovery of TER development in the transfected cells following Zn^{++} induction TER depression. Cells were treated in an identical fashion to those in figure 12. Unlike Zn^{++}-treated transfected cells, Zn^{++} untreated transfected and untransfected controls develop a higher TER more rapidly. Zn^{++} removal after 24 hours (arrow), however, shows transfected cells to undergo a normal TER development, indicating that cell mortality was not the cause of depressed TER values.

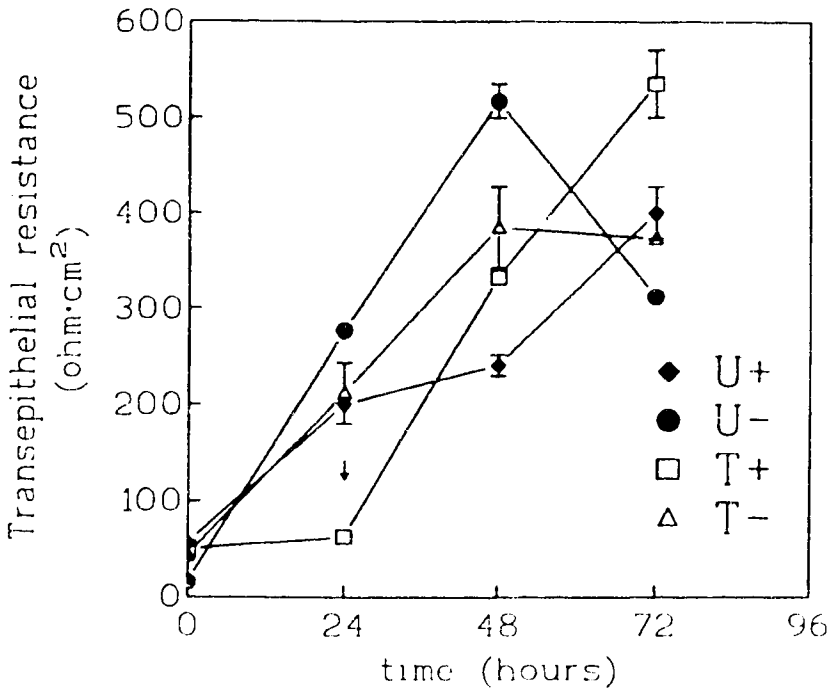
Transepithelial resistance
(ohm·cm²)
600
500
400
300
200
100
0
0
24
48
72
96
time (hours)
U+
U−
T+
T−

Figure 14. One experiment showing TER values and corresponding ZO-1 protein levels of Zn^{++}-induce or Zn^{++}-uninduced transfected and untransfected cells switched to normal Ca^{++} medium in the presence or absence or Zn^{++}. Cells were treated identically to those in figure 12 and were harvested for protein after 48 hours. a) Untransfected cells grown with (U+) or without (U-) Zn^{++} and transfected cells grown with (T+) or without (T-) Zn^{++} are shown. Zn^{++}-treated transfected cells TER values are significantly lower than other controls at 48 hours. b) Autoradiograph of a western blot of ZO-1 isolated from duplicate cell filters treated as in part a. Protein was isolated at the 48 hour time point. ZO-1 protein levels of Zn^{++}-treated A1 cells are observably lower than other controls and correlate with a lower TER value. c) Graph of the corresponding ^{125}I-quantified ZO-1 protein amounts from figure 14b. Averaged ^{125}I-quantified ZO-1 protein values from duplicate filters were graphed. Lower protein values support observed differences in the ZO-1 protein content seen in figure 14b. Protein and TER data suggest that a lack of ZO-1 protein is correlated with a decrease in TER. d) Graph of ^{125}I-quantified ZO-1 protein from a western blot of increasing volumes of MDCK cell lysate. By loading 10, 20, 30, 40, and 50 μl of lysate a linear range of between 0 and 2500 cpm was achieved and used to define the linear range for all quantitative western blots done in this work.

a

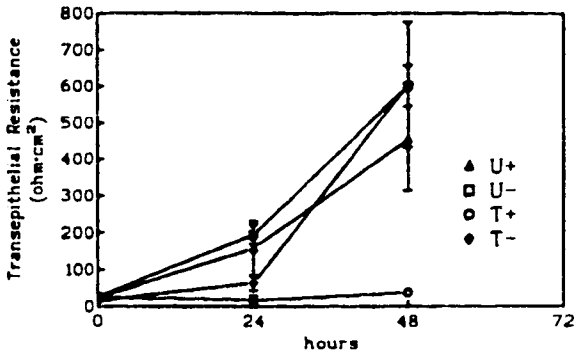
Transepithelial Resistance (ohm·cm²)
800
700
600
500
400
300
200
100
0
0
24
48
72
hours
U+
U-
T+
T-

b

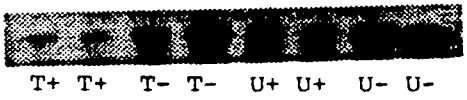
T+ T+ T- T- U+ U+ U- U-

c

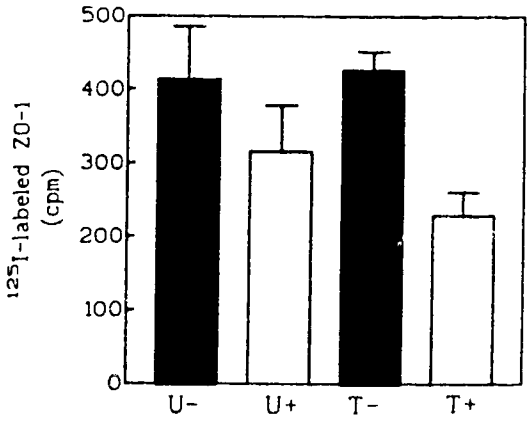
125I-labeled ZO-1 (cpm)
500
400
300
200
100
0
U-
U+
T-
T+

d

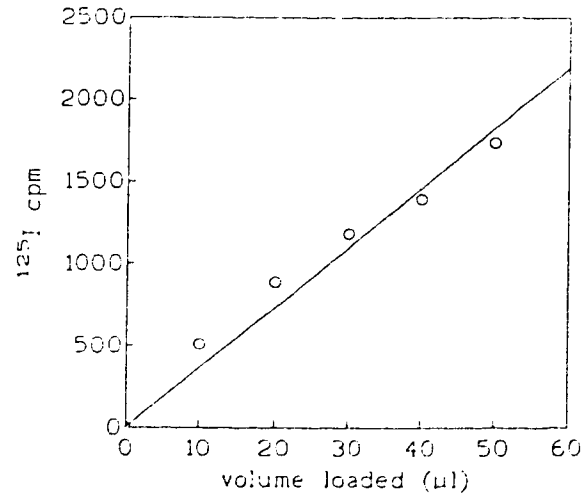
125I cpm
2500
2000
1500
1000
500
0
0
10
20
30
40
50
60
volume loaded (µl)

Figure 15. One experiment showing a rapid increase in TER following Zn^{++} treatment of transfected cells relative to controls. Cells were treated identically to those in figure 12, were monitored for 24 hours and then protein harvested. a) TER values of Zn^{++}-induced or Zn^{++}-uninduced transfected and untransfected cells. Untransfected cells grown with (U+) or without (U-) Zn^{++} and transfected cells grown with (T+) or without (T-) Zn^{++} are shown. TER values of Zn^{++}-treated A1 cells are significantly higher than other controls. b) Western blot of ZO-1 protein isolated from the Zn^{++}-treated or -untreated MDCK and A1 cells in figure 15a. Protein was isolated from identically treated duplicate filters from each of the four conditions: A1 cells grown in the presence (T+) or the absence (T-) of Zn^{++} or MDCK cells grown in the presence (U+) or absence (U-) of Zn^{++}. ZO-1 protein levels of Zn^{++}-treated A1 cells are observably higher than other controls and correlate with the higher TER values. c) Graph of the corresponding ^{125}I-quantified ZO-1 protein amounts from figure 15b. Averaged ^{125}I-quantified ZO-1 protein values from duplicate filters were graphed. Coincidental increased ZO-1 protein levels and TER values suggests that there is a role for ZO-1 protein in the process of TER development.

a

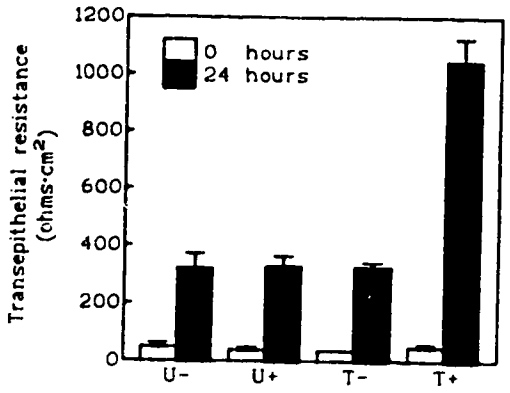
Transepithelial resistance (ohms·cm²)
1200
1000
800
600
400
200
0
0 hours
24 hours
U-
U+
T-
T+

b

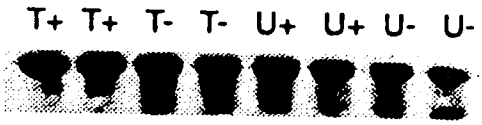
T+ T+ T- T- U+ U+ U- U-

c

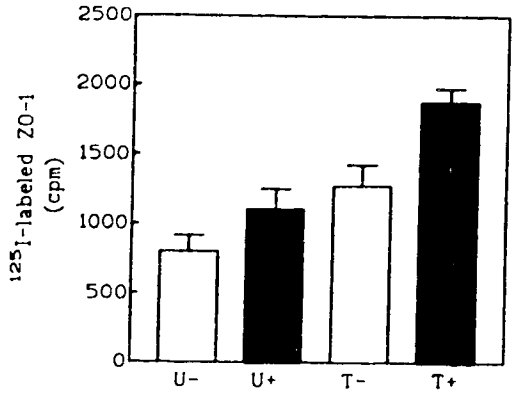
125I-labeled ZO-1 (cpm)
2500
2000
1500
1000
500
0
U-
U+
T-
T+

BIBLIOGRAPHY

Anderson, J., C. Itallie, M. Peterson, B. Stevenson, E. Carew, and M. Mooseker. (1989) J. Cell Biol. 109: 1047-1056.

Anderson, J., Stevenson, B., Jesaitis, L., Goodenough, D., and Mooseker, M. (1988) J. Cell. Biol. 106: 1141-1149.

Ausubel F., Brent R., Kingston R., Moore D., Smith J., Seidmen J., Struhl K. Current Protocols in Molecular Biology. (1991) Wiley Interscience, New York.

Balda M., Gonzalez-Mariscal L., Contreras R., Macias-Silva M., Torres-Marquez E., Garcia Sainz A., Cereijido M. (1991) J. Memb. Biol. 122: 193-202.

Balda MB, Gonzalez-Mariscal I, Matter K, Cereijido M, Anderson JM. (1993) J. Cell Biol.

Bass L. and Weintraub H. (1987) Cell. 48: 607-613

Caplan M., Matlin K. (1989) In: Functional Epithelial Cells in Culture. Matlin K., ed., Liss, New York. pp71-127.

Cereijido M., Meza I., Martinez-Paloma A. (1981) Am. J. Physiol. 240: 96-102.

Chevalier j., Pinto da Silva P., (1987) J. Membr. Biol. 95: 199-208.

Chomcynski P., Sacchi N. (1987) Anal. Biochem. 156-162.

Citi S., Sabanay R., Jakes R., Geiger B., Kendrick-Jones J. (1988) Nature. 333: 272-276.

Citi S. (1992) J. Cell Biol. 117: 169-178.

Claude P., Goodenough D. (1973) J. Cell Biol. 58: 390-400.

Diamond J. (1977) Physiologist. 20: 10-18.

Fernandez J., Geiger B., Salomon D., Ben-Ze'ev A. (1993) J. Cell Biol. 122: 1285-1294.

Furuse M., Tetsuaki H., Itoh M., Nagafuchi A., Yonemura S., Tsukita S., Tsukita S. (1993) J. Cell Biol. 123: 1777-1788.

Gonzales-Mariscal L., Contreras J., Bolivar A., Ponce B., Chavez De Ramirez., Cereijido M. (1990) Am. J. Phsiol. 259: 978-986.

Griepp E., Dolan E., Robbins S., Sabatini D. (1983) J. Cell Biol. 96: 693-702.

Gumbiner B., Simons K. (1986) J. Cell Biol. 102: 457-468.

Gumbiner B., Stevenson B., Grimaldi A. (1988) J. Cell Biol. 107: 1575-1587.

Gumbiner B., Lowenkopf T., Apatira D. (1991) Proc. Natl. Acad. Sci. USA. 88: 3460-3464.

Howarth, A., Hughes, M., and Stevenson, B. (1992) Am. J. Physiol. 262: 461-469.

Howarth A., Singer K., Stevenson B. (1994) J. Memb. Biol. 137: 261- 270.

Itoh M., Yonemura S., Nagafuchi A., Tsukita S., Tsukita S. (1991) J. Cell Biol. 115: 1449-1462.

Itoh M., Nagafuchi A., Yonemura S., Kitani-Yasuda T., Tsukita S., Tsukita S. (1993) J. Cell Biol. 121: 491-502.

Kachar B., Pinto da Silva P. (1981) Science. 213: 541-544.

Kartenbeck J., Schmelz M., Franke W., Geiger B. (1991) J. Cell Biol. 113: 881-892.

Kleppe, K., Ohtsuka, E., Kleppe, R., Molineux, I., and Khorana, H. (1971) Mol Biol. 56: 341-361.

Knecht D., Loomis W. (1987) Science. 236: 1081-1086.

Knecht D. (1989) Cell Motil. Cytoskel. 14: 92-102.

Kurihara H., Anderson J., Kerjaschki D., Farquhar M. (1992) Am. J. Pathol. 141: 805-816.

Liu, T., Williams J., Clarke M. (1992) Mol. Biol. Cell. 3: 1403-1413.

Madara J., Dharmasthaphorn K. (1985) J. Cell Biol. 101: 2124-2133.

Madara J., Barenberg D., Carlson S. (1986) J. Cell Biol. 102: 2125-2136.

Madara J. (1987) Am. J. Physiol. 253: 121-175.

Mege, R. M., Matsuzaki F., Gallin W.J., Goldberg J.I., Cunningham B.A., and Edelman G.M. (1988). Proc. Natl. Acad. Sci. U.S.A.. 85: 7274-7278.

Meza, I., G. Ibarra, M. Sabenero, A. Martinez-Palomo, and M. Cereijido. (1980). J. Cell Biol. 87: 746-754.

Meza I., Sababero E., Stefani M., Cereijido M. (1982) J. Cell. Biochem. 18: 407-421.

Nigam S., Denisenko N., Rodriguez-Boulan E., Citi S. (1991) Biochem. Biophys. Res. Commun. 181: 548-553.

Pitelka D., Taggart N., Hamamoto S. (1983) J. Cell Biol. 96: 613-624.

Pinto da Silva P., Kachar B. (1982) Cell. 28: 441-450.

Rothman J., Orci L. (1990) FASEB J. 4: 1460-1468.

Saiki, R., Bugawan, T., Horn, G., Mullis, K., and Erlich, H. (1986) Nature (Lond.). 324: 163-166.

Sanger F., Nicklen S., Coulson A. (1977) Proc. Natl. Acad. Sci. U.S.A.. 74: 5463-5467.

Sanger F., Coulson A., Barrell B., Smith A., Roe B. (1980) J Mol. Biol. 143: 161-178.

Sedar A., Forte J. (1964) J. Cell Biol. 22: 173-188.

Schulze H., Huckriede A., Noegel A., Schleicher M., and Jockush B. (1989) EMBO. 8: 3587-3593.

Staehelin L. (1973) J. Cell Sci. 13: 763-786.

Staehelin L. (1974) Int. Rev. Cytol. 39: 191-282.

Stevenson B., Goodenough D., (1984) J. Cell Biol. 98: 1209-1221.

Stevenson B., Sicliciano J., Mooseker M., Goodenough D., (1986) J. Cell Biol. 103: 755-766.

Stevenson B., Begg. D. (1994) J. Cell Sci. in press

Tabor S., Richardson C. (1990) J. Biol. Chem. 265: 8322-8328.

van der Krol A., Lenting P., Veenstra J., van der Meer I., Koes R., Gerats A., Mol J., Stuitje A. (1988) Biotechniques. 6: 958-976.

Verkliej A. (1984) Biochim. Biophys. Acta. 779: 43-63.

Volberg T., Geiger B., Kartenbeck J., Franke W. (1986) J. Cell Biol. 102: 1833-1842.

Willot E., Balda S., Heintzelman M., Jameson B., Anderson J. (1992) Am. J. Physiol. 263: C1119-C1122.

Willot E., Balda M., Fanning A., Jameson B., Van Itallie C., Anderson J. (1993) Proc. Natl. Acad. Sci. USA. 90: 7834-7838.

Woods D., Bryant P. (1991) Cell. 66: 451-464.

Zhong Y., Saitoh T., Minase T., Sawada N., Enomoto K., Mori M. (1993) J. Cell Biol. 120: 477-483.

Zahraoui A., Gerard J., Monique A., Fontaine J., Hellio R., Tavitian A., Louvard D. (1994) J. Cell Biol. 124: 101-115.